

EA MAXIJ 1820+070

Karan Kumar B Project

University of Amsterdam 2023

1 Contributions

Karan and Syarief both worked on the Section 2 and the code. Sections 3 and 4 and verification are individual.

2 Introduction

MAXI J1820+070 is a low mass x-ray binary system. During 2018 multiple outbursts were detected in the hard state [Bright et al. \(2020\)](#); [Atri et al. \(2020\)](#). It is hypothesized that emission in the hard state is dominated by the corona and generates a non-thermal X-ray spectrum [Bright et al. \(2020\)](#). Our interest is in the corona of the black hole during the hard state, we model and verify the cyclo/synchrotron emission, synchrotron self-Compton scattering and inverse self-Compton of the black-body into the corona. Table 1 shows our free parameters from literature [Chakraborty et al. \(2020\)](#); [Rodi et al. \(2021\)](#); [Atri et al. \(2020\)](#).

3 Cyclotron and Synchrotron

Our process is similar for both Cyclotron and Synchrotron emission. Following our work from assignments 3 and 5 in class we treat the corona as a spherical blob at constant radius size ($10r_g$).

From equipartition we assume $U_e = U_b$ to calculate the C and \hat{C} constants. Our equations to evaluate the constants are given in equation 1.

$$\begin{aligned}\hat{C} &= \frac{U_e}{\int E^{-p+1} dE} \\ C &= \frac{\hat{C}}{m_e c^2} \\ U_e &= \frac{\eta L_{edd}}{4\pi R_0^2 v_r} \\ U_b &= \frac{B^2}{8\pi}\end{aligned}\tag{1}$$

Where η and v_r are free parameters of efficiency and electron velocity respectively. Thanks to Ben and Leon we know that for a Maxwell-Juttner distribution in the corona, the power law approximates as $p=4$. We

Table 1: Table of parameters from literature

B (G)	$1.6 \cdot 10^6$
M (M_\odot)	9.2
η	0.15
γ_{max}	1000
$R_0(r_g)$	10
$v_r(c)$	0.89
$L_{edd}(ergs/s)$	10^{39}
Distance (kpc)	2.96

use C , \hat{C} and the magnetic field to evaluate the source function in terms of the emission n_ν and absorption coefficient α_ν .

$$S_\nu = \frac{n_\nu}{\alpha_\nu} \quad (2)$$

Where α_ν is the absorption coefficient defined in chapter 6 of [Rybicki & Lightman \(1986\)](#), We apply this absorption coefficient in both the cyclotron and synchrotron spectrum, subsections 3.1 and 3.2 have expressions for their respective emission coefficients. The intensity I_ν and flux F_ν measured at earth is given by equation 3. We assume the corona is spherical and at the base of jet therefore we calculate the intensity and flux for one slice at the base of the jet.

$$I_\nu = S_\nu(1 - e^{-\tau})$$

$$F_\nu = I_\nu \left(\frac{R^2}{D^2} \right) \quad (3)$$

We apply this to both the cyclotron emission and synchrotron emission to plot a flat jet spectrum as shown in figure 1.

3.1 Cyclotron Emission

Beginning with the non-radiative emission, cyclotron emission comes from the gyration of charged particles around a magnetic field [Rybicki & Lightman \(1986\)](#). We treat the corona as the base of the jet in the hard state, and charged particles enter the system through this base. The spectrum model follows the steps in [Lucchini et al. \(2022\)](#) in the frame of the corona. To account for relativistic and non-relativistic effects we define an electron distribution $N(\gamma)$ in terms of non-dimensional momentum (ρ), see [Lucchini et al. \(2022\)](#); [Katarzyński et al. \(2006\)](#)

$$N(\gamma) = N(\rho) \frac{d\rho}{d\gamma} \quad (4)$$

$$\gamma(\rho) = \sqrt{\rho^2 + 1}$$

$$N(\rho) = N_o \rho^2 e^{-\frac{\gamma(\rho)}{\theta}} \quad (5)$$

Where $N(\rho)$ is the Maxwell–Jüttner distribution and $\theta = \frac{K_b T}{m_e c}$ is the dimensionless thermal temperature of the electrons [Lucchini et al. \(2022\)](#). The total cyclotron emissivity is given by [Lucchini et al. \(2022\)](#) as

$$j_c(\nu) = \int_{\gamma_{min}}^{\gamma_{max}} N(\gamma) j_c(\nu, \gamma) d\gamma \quad (6)$$

Where $j_c(\nu, \gamma)$ is the emissivity per particle with Lorentz factor γ [Lucchini et al. \(2022\)](#).

For non-relativistic emission we calculate the spectrum in terms of the Larmor frequency

$$\nu_l = \gamma^2 \frac{qB}{2\pi m_e c} \quad (7)$$

Where the Lorentz factor is between 1.1 and 2.0 for cyclotron emission [Lucchini et al. \(2022\)](#)

3.2 Synchrotron Self Absorption

Synchrotron emission comes from the radiation produced by relativistic particles in a magnetic field. We assume the corona is an isotropic source of this radiation. The emission of photons falls between the characteristic frequency regime as:

$$\nu_c = \frac{3\gamma^2}{4\pi} \omega_g \sin(\alpha) = 4.3 \cdot 10^6 B \gamma^2 H z \quad (8)$$

Where B is the magnetic field strength in Gauss [Rybicki & Lightman \(1986\)](#), We calculate a minimum and maximum characteristic frequency in terms of $\gamma_{min} = 2$ and $\gamma_{max} = 1000$. Initially we wished to follow the steps in [Lucchini et al. \(2022\)](#) to calculate synchrotron emissivity and absorption but had errors deriving the integrals. We therefore follow assignment 5 and calculate the synchrotron spectrum as one slice of the jet for $p=4$. Thanks to Ben and Leon for the advice. The procedure to calculate the spectrum is outlined in section 3. Following chapter 6 and equation 6.36 in [Rybicki & Lightman \(1986\)](#) to calculate the total emission for arbitrary p indices.

4 Compton Scattering

Radiation from Compton scattering comes from seed photons that scatter with an electron and the photon gains energy. In the rest frame of the electron we assume the photon's energy is much less than the rest energy of the electron and therefore the probability of collision is related by the Thompson cross section [Rybicki & Lightman \(1986\)](#). In our model the source of the electrons come from the corona. We consider two sources of photons for Compton scattering. The first are photons from the black-body disk which enter the corona and undergo Compton scattering; the second are photons from the corona produced by synchrotron radiation. In both cases we assume a constant optical depth $\tau = 0.1$

Figure 5 Shows a Maxwell-Juttner distribution.

$$f(\gamma) = \frac{\gamma^2 \beta(\gamma)}{\theta K_2(\frac{1}{\theta})} e^{-\frac{\gamma}{\theta}} \quad (9)$$

For both black-body and SSC we compile a Maxwell Juttner distribution from equation 9 in terms of γ_{min} and γ_{max} . We create a probability distribution function and sample a Lorentz factor and convert this into a velocity to input in the Monte Carlo simulation. The velocity is given by equation 10.

$$v_{samp} = \sqrt{1 - \frac{1}{\gamma_{samp}^2}} c \quad (10)$$

4.1 SSC from the Corona

To create a photon spectrum from our corona. We create a photon density distribution following chapter 7 in [Rybicki & Lightman \(1986\)](#). From the intensity of the corona, we create a probability density function for photon frequency. The distribution is provided in figure 3. From the sample the energy of the photons is simply $E = h\nu$ and select one random energy. We pass this energy with our Maxwell juttner distribution into the Monte Carlo simulation to create our spectrum for SSC.

4.2 Inverse Compton from the Black-body

We treat the photons from the accretion disk as a black-body with constant kT and collide with electrons in the corona with a Maxwell-Juttner distribution. The photons follow a Planck distribution straight from the MC tutorial [Sebastian Heinz \(2023\)](#), and parameterized in terms of kT_e kT_{seed} and height of the corona H We obtain values for this from literature [Chakraborty et al. \(2020\)](#) as $kT_e = 150 \text{ KeV}$ $kT_{seed} = 0.3 \text{ KeV}$ and $H = 8r_g$.

5 Verification

1. Flux: Comparing our synchrotron flux in figure 1 to [Rodi et al. \(2021\)](#), when we treat the corona as the base of the jet our flux is within one order of magnitude, showing our spectrum is within agreement with the jet model. And our assumption of $p=4$ remains valid. Although our cutoff frequency at 10^{18} Hz is much larger compared to [Rodi et al. \(2021\)](#). (see fig 4).
2. Equipartition: Assuming equipartition we calculate the magnetic field strength in the Corona from [Rybicki & Lightman \(1986\)](#) and equation 1.

$$\begin{aligned} U_B &= U_e \\ B &= \sqrt{4\pi U_b} \end{aligned} \quad (11)$$

We calculate magnetic field strength of order $10^{15} G$ so much larger than the reported field strength of $B = 10^6 G$ by [Rodi et al. \(2021\)](#). Clearly our assumption for efficiency, radius or velocity of the corona is wrong. If we calculate efficiency using $B = 10^6 G$, the efficiency should be of order $\eta = 10^{-4}$. An OOM calculation is shown below.

$$\begin{aligned}
U_B &= \frac{B^2}{8\pi} = 10^{12} \frac{\text{ergs}}{\text{cm}^3} \\
\eta &= \frac{U_B(4\pi R_0^2 v_r)}{L_{\text{edd}}} = \frac{10^{12+14+9}}{10^{39}} \\
\eta &= 10^{-4}
\end{aligned} \tag{12}$$

3. Compton y and $\langle \gamma^2 \rangle$: The Maxwell Juttner distribution accounts for relativistic velocities as well as non-relativistic. In the corona we expect an extremely relativistic velocity distribution in the hard state of the jet [Bright et al. \(2020\)](#) and a large y-parameter, greater than one. For both the black-body and SSC the y-parameter was greater than one, implying that the photons gained a non-negligible amount of energy in the rest frame of the corona. [Rybicki & Lightman \(1986\)](#)

Double checking in terms of energy:

$$Y = \frac{\Delta E}{E_0} = \langle \gamma^2 \rangle \tag{13}$$

In the relativistic case. $\langle \gamma^2 \rangle$ is of order 10^{4-6} [Rybicki & Lightman \(1986\)](#) In figure 1 and 2. The peak frequencies lie at 10^{14} and 10^{18} Hz respectively. implying $\langle \gamma^2 \rangle = 4$ if we use IC, this means on average the photons gain a factor 10^4 energy per scatter. Although this value is within the lower limits i am skeptical since it only shows for IC for the black-body and not our corona-jet model. Additional our MC spectrum isn't accurate, this is described in the "Monte Carlo Sim" verification.

4. SSA peak: Checking the peak of synchrotron self-absorption figure fig:SSA and comparing to [Rodi et al. \(2021\)](#) who report $\nu_{ssa} = 10^{14} \text{Hz}$ we note our peak SSA is of same order. Initially we were two orders of magnitude too large. Reading [Rodi et al. \(2021\)](#) I thought that the power law index fit could account for the two orders of magnitude difference. We assume for synchrotron radiation is fixed at $p=4$ for an optically thin corona. However, [Rodi et al. \(2021\)](#) models a best fit for an optically thin jet at $p=2.1$. But this should only affect the steepness of the curve, not where the peak lies. We corrected for the two orders of magnitude error by reviewing the units of our equitation function. (see equation 1, 11).

5. Monte Carlo Sim: In figure 2 We include both parts of the spectrum and follow the steps outlined in section 4 and input parameters from [Chakraborty et al. \(2020\)](#). The IC and SSC data is not flux rather it is number of photons, the default output from the monte carlo simulation [Sebastian Heinz \(2023\)](#). On paper we know to convert number of photons into intensity as

$$I_\nu = \frac{\text{number}}{\text{sec}} \frac{h\nu}{\Delta\nu} \frac{1}{4\pi d^2} \tag{14}$$

And use equation 3 to convert the intensity into a flux. But we were unable to do so. We think the biggest error to this is in our normalization, our flux was reaching order 10^{-70}mJy . Although the frequency bins lie within those seen in literature we cannot say much about the flux because of the normalization. One positive was the y-parameter was always greater than one in our trails. Showing that our Maxwell-Juttner distribution works for relativistic particles.

6. constant tau and Compton hump: In order to see high energy scatters we expected to see a Compton hump as higher frequencies similar to what is shown in figure 4. But this requires a frequency dependent tau, where the frequency is that of the photon being scattered. [Rybicki & Lightman \(1986\)](#). If τ is large, photons will be trapped in the corona as undergo more scatterings, but since we could only get the simulation running for constant $\tau = 0.1$, even if we got the flux we would not see the bump as photons are escaping the corona. A constant optical depth is an oversimplification of the simulation.
7. Electron power law Distribution: We verify we obtain a steep power law curve for the electron distribution, and expect more electrons at lower energies. The electron distribution is given by equation 15

$$n_e = CE^{-p+1} \tag{15}$$

Where n_e is electron density. We sample a distribution and plot it in terms of the electron's momentum in figure 15. Although we verify the shape of the power law it would have been nice to find literature to confirm the numbers or order of magnitude.

6 Conclusion

We attempt to model MAXI J1820+070 a low mass X-ray binary. We model the Corona's spectrum including Cyclotron and Synchrotron, Inverse Compton by the Black-body disk and Synchrotron Self-Compton by the Corona. Following literature parameters we obtain a peak synchrotron frequency that matches literature [Rodi et al. \(2021\)](#) and assuming a power law of $p=4$. Although in verification we find our equipartition does not match. Our Monte Carlo simulation for a maxwell-juttner distribution showed our frequency bins agree on the lower limit and the y -parameter was consistently large. but for many reasons we could not calculate the flux, because of wrong normalization and perhaps too many simplifications.

7 Figures

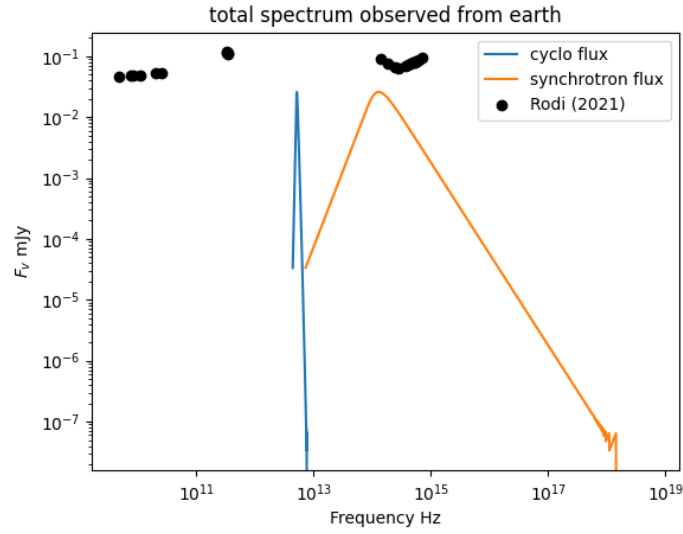


Figure 1: Cyclotron and Synchrotron Spectrum observed from earth. compared with [Rodi et al. \(2021\)](#).

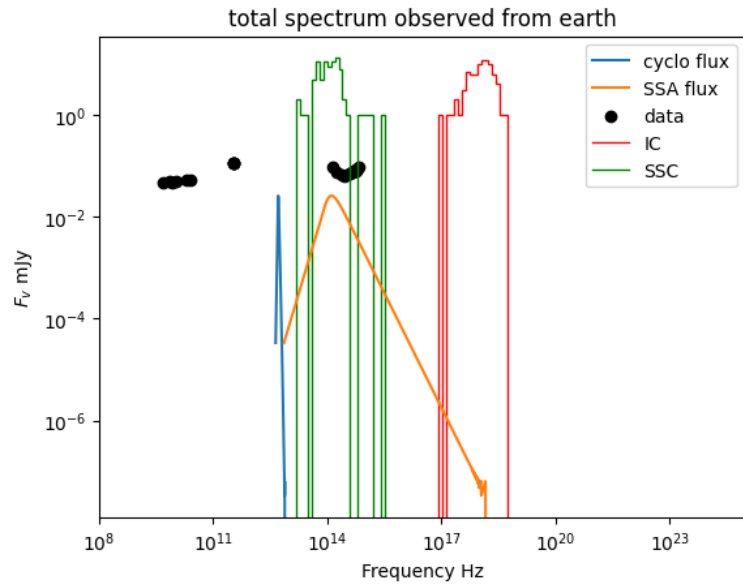


Figure 2: Entire Spectrum including Monte Carlo

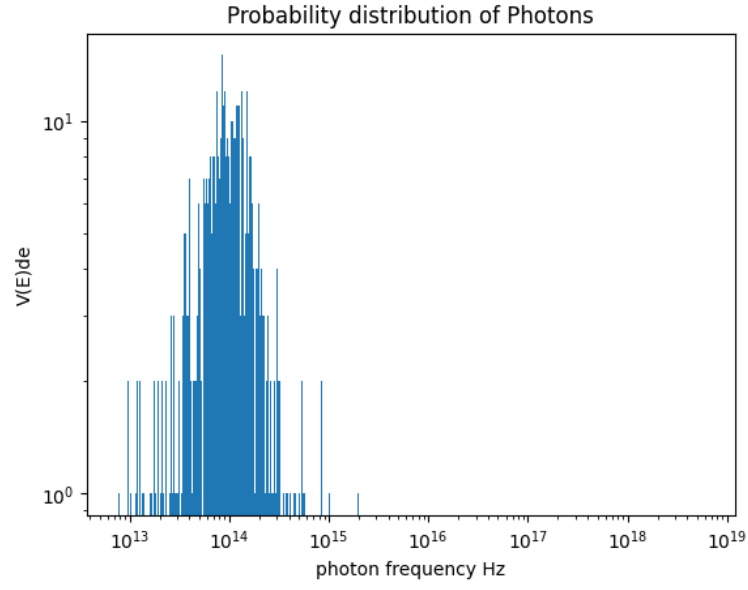


Figure 3: Distribution of Photons, later sampled as input for IC

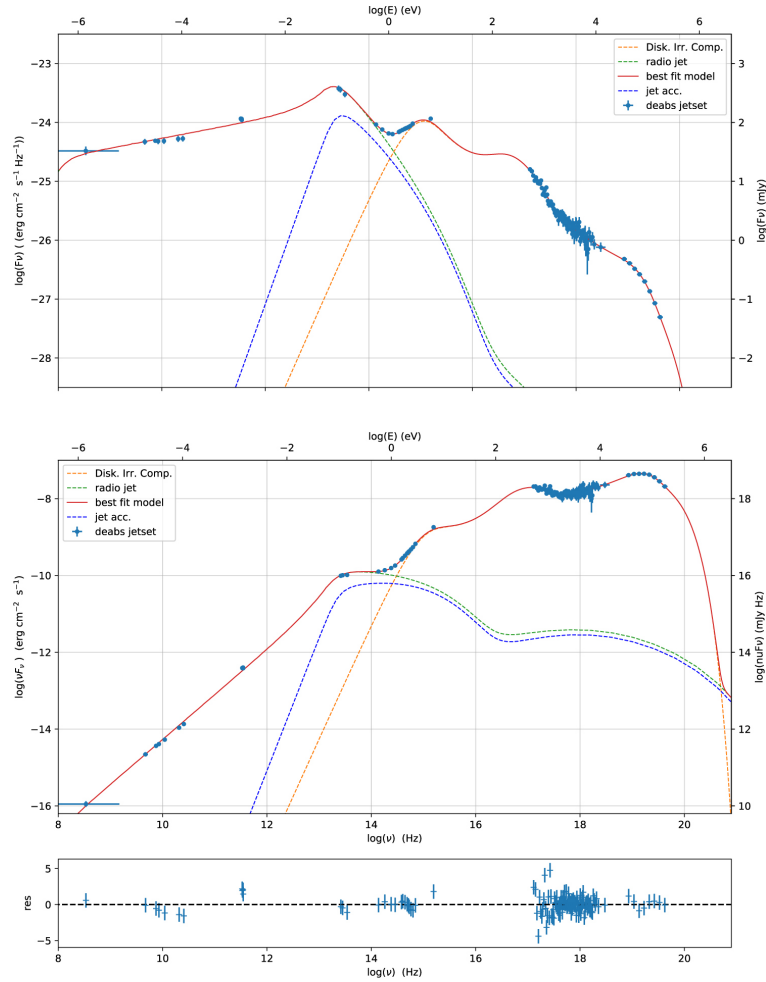


Figure 4: Rodi et al. (2021) Best-fit model of Jet spectrum

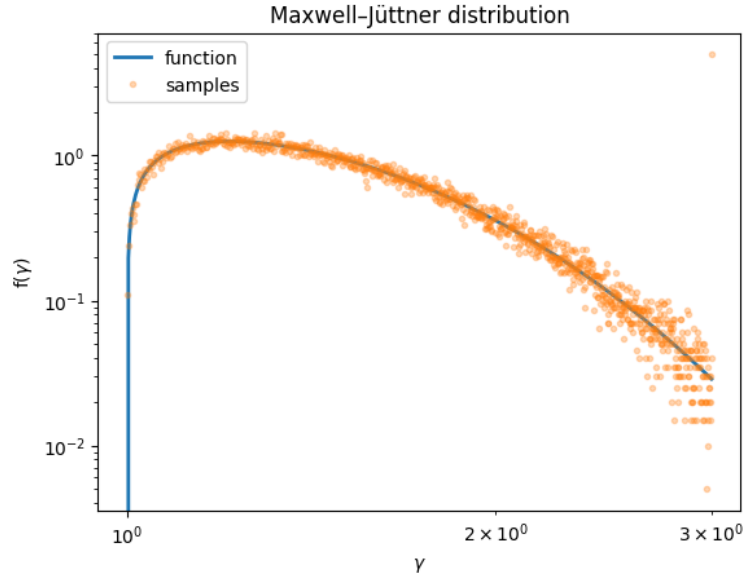


Figure 5: Maxwell-Juttner Distribution

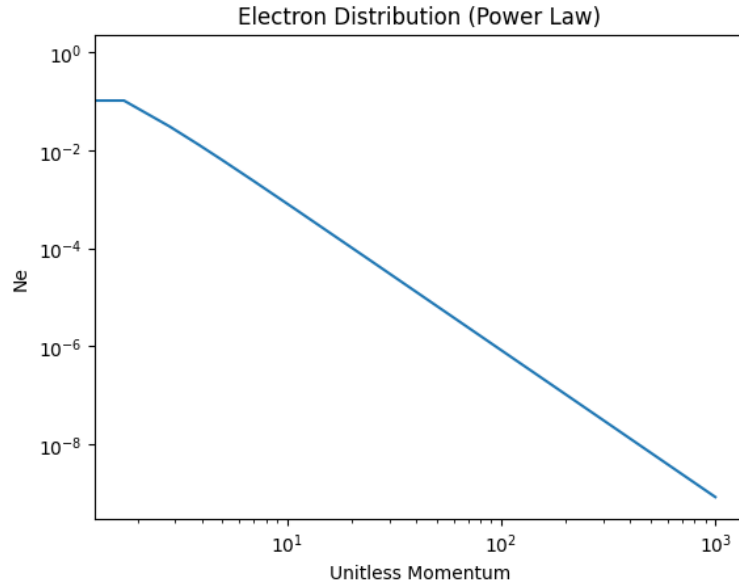


Figure 6: Power law distribution of electrons

References

- Atri, P., Miller-Jones, J. C. A., Bahramian, A., et al. 2020, , 493, L81, doi: [10.1093/mnrasl/slaa010](https://doi.org/10.1093/mnrasl/slaa010)
- Bright, J. S., Fender, R. P., Motta, S. E., et al. 2020, Nature Astronomy, 4, 697, doi: [10.1038/s41550-020-1023-5](https://doi.org/10.1038/s41550-020-1023-5)
- Chakraborty, S., Navale, N., Ratheesh, A., & Bhattacharyya, S. 2020, , 498, 5873, doi: [10.1093/mnras/staa2711](https://doi.org/10.1093/mnras/staa2711)
- Katarzyński, K., Ghisellini, G., Svensson, R., & Gracia, J. 2006, , 451, 739, doi: [10.1051/0004-6361:20054346](https://doi.org/10.1051/0004-6361:20054346)
- Lucchini, M., Ceccobello, C., Markoff, S., et al. 2022, , 517, 5853, doi: [10.1093/mnras/stac2904](https://doi.org/10.1093/mnras/stac2904)

Rodi, J., Tramacere, A., Onori, F., et al. 2021, , 910, 21, doi: [10.3847/1538-4357/abdfd0](https://doi.org/10.3847/1538-4357/abdfd0)

Rybicki, G. B., & Lightman, A. P. 1986, Radiative Processes in Astrophysics

Sebastian Heinz. 2023, Monte-Carlo Inverse Compton Tutorial, version 1.0. <https://www.astro.wisc.edu/staff/heinz-sebastian/>